Supporting Information (SI)

DFT Study on the Mechanism of Methanol Dehydrogenation over Ru_xP_y Surfaces

Hao Lu,[a,] Yuan Zhong,[a,] Yao Jie,[a] Pan Yin,[a] Tian-Yao Shen,[a] Jing-Yi Guo,[a] Wei Zhang,[a] Min Pu,[a] Hong Yan,*[a]

[a] *State Key Laboratory of Chemical Resource Engineering, College of Chemistry, Beijing University of Chemical Technology, Beijing 100029, China*

***** Corresponding Authors:

yanhong@mail.buct.edu.cn (Hong Yan).

Contents

1.The structures of Ru, Ru_2P, RuP, RuP_2 unit cells.

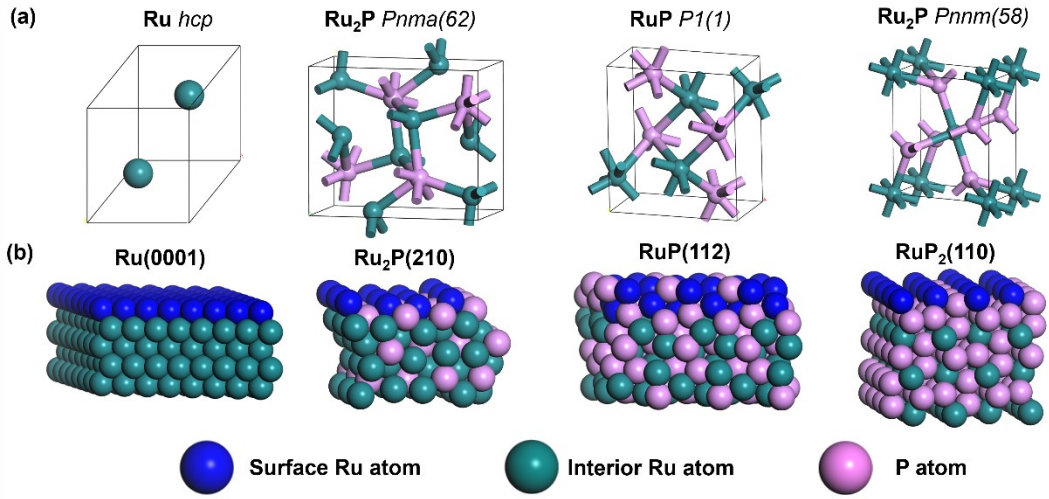

Figure S1. (a) Structure model of Cells. (b) Structures of Ru(0001), Ru_2P(210), RuP(112), and RuP_2(110).

2. Energy test for K-point.

As shown in Table S1, when the K-point is set to 3×3×1, the adsorption energy (The test site is not the optimal adsorption site) is -0.565 eV, and when the K-point is increased to 5×5×1, the DFT calculation results show that the adsorption energy has only a small change (0.001 eV). Therefore, in order to save computing resources, the K-point of 3×3×1 is used to complete all calculations.

Table S1. Adsorption energy of Propane molecules on RuP(112) surface when K-point are 3×3×1 and 5×5×1(in eV).

K-pont	$E_{surface}$	$E_{adsorbate}$	$E_{adsorbate/surface}$	E_{ads}
3×3×1	-229.549	-57.012	-287.126	-0.565
5×5×1	-229.549	-57.012	-287.127	-0.566

3. Energy test for cut-off energy (ENCUT).

In order to make reasonable use of computing resources, we tested the cutoff energy (ENCUT) required for the calculation. If the ENCUT value is too small, the

system will be difficult to converge, and if it is too large, it will take longer to waste computing resources. As shown in Figure S2, for the system we want to study, when the ENCUT value is 450 eV, it can not only ensure the convergence of the system, but also save computing resources.

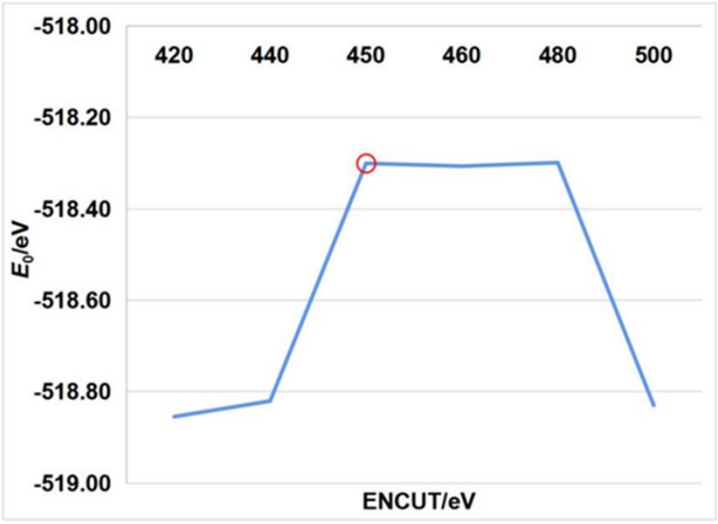

Figure S2. Take the energy E_0 of CH_3OH adsorbed on RuP(112) surface as an example for ENCUT test.

2. Energy test for the energy convergence criterion.

As shown in Table S2, when the energy convergence criterion is set to 0.05 eV/Å, the adsorption energy is -0.6185 eV, and when the energy convergence criterion is decreased to 0.02 eV/Å, the DFT calculation results show that the adsorption energy has only a small change (0.0012 eV). Therefore, in order to save computing resources, the energy convergence criterion of 0.05 eV/Å is used to complete all calculations.

Table S2. Adsorption energy of methanol molecules on RuP_2(110) surface when energy convergence criterion are 0.02 and 0.05 (in eV/ Å).

EDIFFG	$E_{surface}$	$E_{adsorbate}$	$E_{adsorbate/surface}$	E_{ads}
0.02 eV/Å	-492.3153	-30.2068	-523.1406	-0.6185
0.05 eV/Å	-492.3167	-30.2073	-523.1413	-0.6173

4.Adsorption information for MD reaction intermediates on Ru(0001), Ru_2P(210), RuP(112), and RuP_2(110).

Table S3. Adsorption sites, adsorption energies (in eV), and structural parameters (in angstroms) for intermediates involved in MD on Ru(0001).

Species	Sites	Configuration	E_{ads}/eV	d_{C-O}/Å	d_{C-H}/Å	d_{O-H}/Å	d_{C-Ru}/Å	d_{O-Ru}/Å
CH_3OH*	Ru-top	η^1(O)	-0.482	1.450	1.100	0.980		2.306
CH_2OH*	Ru_2-bridge	η^1(C)–η^1(O)	-1.857	1.476	1.100	0.981	2.145	2.271
CH_3O*	Ru_3-fcc	η^3(O)	-2.666	1.437	1.100			2.166, 2.202, 2.254
CH_2O*	Ru_3-hcp	η^1(C)–η^2(O)	-1.020	1.414	1.104		2.146	2.167, 2.192
CHOH*	Ru_3-hcp	η^2(C)–η^1(O)	-3.054	1.469	1.102	0.983	2.104, 2.085	2.273
CHO*	Ru_2-bridge	η^2(O)	-2.420	1.269	1.113		2.010	2.196
COH*	Ru_3-fcc	η^3(O)	-4.299	1.349		0.981	2.094, 2.045, 2.030	
CO*	Ru-top	η^1(C)	-1.771	1.167			1.902	

Table S4. Adsorption sites, adsorption energies (in eV), and structural parameters (in angstroms) for intermediates involved in MD on Ru_2P(210).

Species	Sites	Configuration	E_{ads}/eV	d_{C-O}/Å	d_{C-H}/Å	d_{O-H}/Å	d_{C-Ru}/Å	d_{O-Ru}/Å
CH_3OH*	Ru-top	η^1(O)	-0.634	1.445	1.100	0.978		2.309
CH_2OH*	Ru_2-bridge	η^1(C)–η^1(O)	-1.884	1.466	1.101, 1.099	0.981	2.135	2.242
CH_3O*	Ru-top	η^1(O)	-2.403	1.407	1.109, 1.107, 1.104			1.954
CH_2O*	Ru_2-bridge	η^1(C)–η^1(O)	-0.793	1.368	1.102		2.254	1.967
CHOH*	Ru-top	η^1(C)	-2.376	1.335	1.106	0.994	1.932	

CHO*	Ru_2-bridge	η^1(C)–η^1(O)	-2.386	1.283	1.110		2.062	2.098
COH*	Ru-top	η^1(O)	-3.986	1.294		0.985	1.762	
CO*	Ru-top	η^1(O)	-1.784	1.171			1.868	

Table S5. Adsorption sites, adsorption energies (in eV), and structural parameters (in angstroms) for intermediates involved in MD on RuP(112).

Species	**Sites**	**Configuration**	E_{ads}/eV	$d_{C–O}$/Å	$d_{C–H}$/Å	$d_{O–H}$/Å	$d_{C–Ru}$/Å	$d_{O–Ru}$/Å
CH_3OH*	Ru-top	η^1(O)	-0.673	1.445	1.100	0.980		2.225
CH_2OH*	Ru-top	η^1(C)	-2.352	1.423	1.095, 1.093	0.988	2.084	
CH_3O*	Ru-top	η^1(O)	-2.533	1.407	1.106, 1.105, 1.104			1.928
CH_2O*	Ru-bridge	η^1(C)–η^1(O)	-0.990	1.331	1.108, 1.102		2.124	2.040
CHOH*	Ru_2-bridge	η^2(C)	-2.848	1.361	1.112	0.994	2.086, 2.054	
CHO*	Ru_2-bridge	η^1(C)–η^1(O)	-2.913	1.287	1.110		2.107, 2.050	
COH*	Ru_2-bridge	η^2(C)	-3.878	1.322		0.982	1.967, 1.917	
CO*	Ru_2-bridge	η^2(O)	-1.282	1.193			2.078, 1.992	

Table S6. Adsorption sites, adsorption energies (in eV), and structural parameters (in angstroms) for intermediates involved in MD on RuP_2(110).

Species	**Sites**	**Configuration**	E_{ads}/eV	$d_{C–O}$/Å	$d_{C–H}$/Å	$d_{O–H}$/Å	$d_{C–Ru}$/Å	$d_{O–Ru}$/Å
CH_3OH*	Ru-top	η^1(O)	-0.617	1.451	1.100	0.992		2.290
CH_3O*	Ru_2-bridge	η^2(O)	-2.814	1.427	1.104, 1.103, 1.102			2.168, 2.180

CH_2OH*	Ru-top	η^1(O)	-0.479	1.372	1.085, 1.084	0.997		2.354
CH_2O*	Ru_2-bridge	η^2(O)	-1.027	1.247	1.103, 1.102			2.284, 2.340
CHO*	Ru_2-bridge	η^1(C)–η^1(O)	-2.100	1.265	1.116		2.046	2.228
CO*	Ru-top	η^1(C)	-1.248	1.162			1.925	

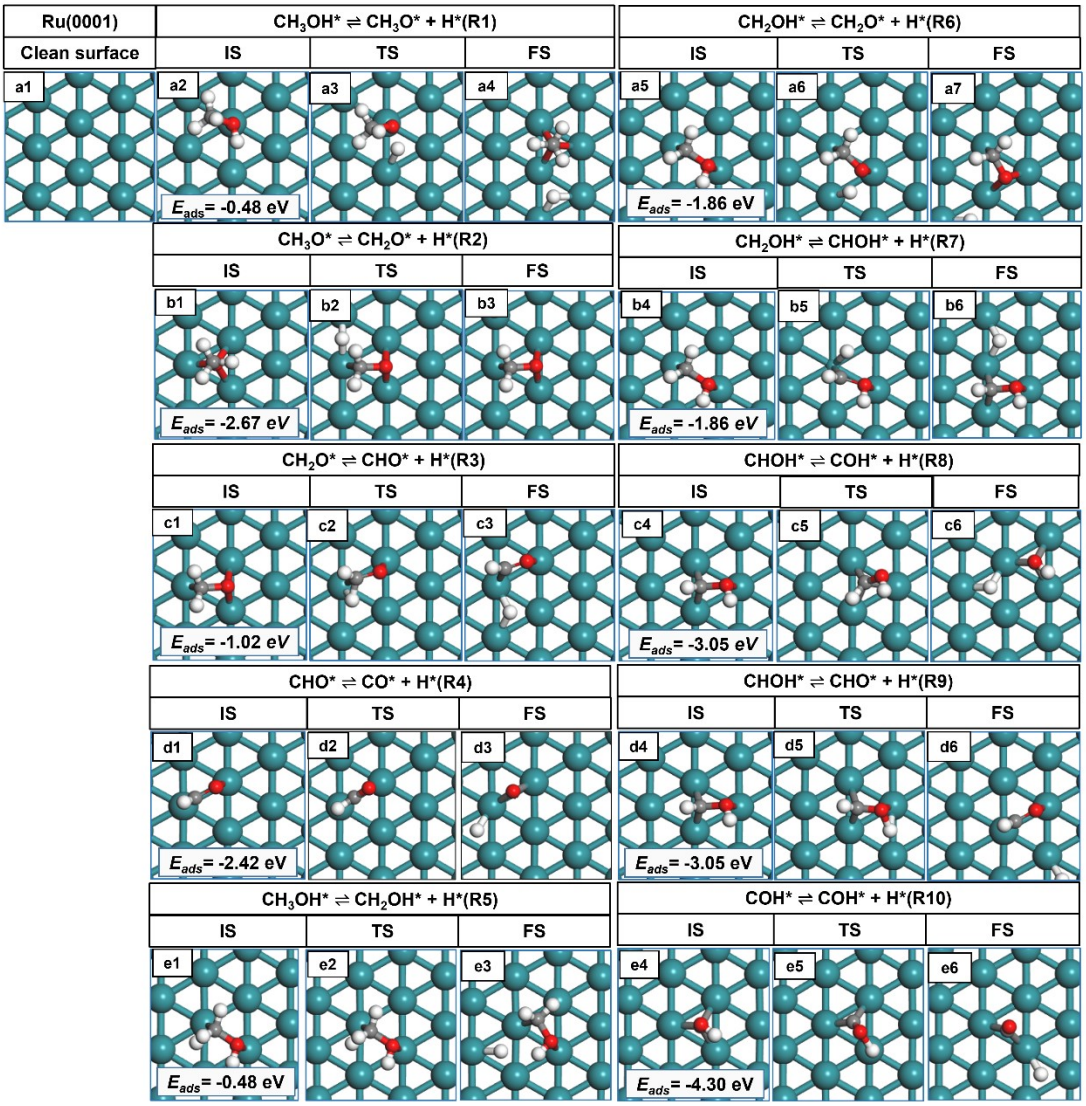

Figure S3. Top view of all the initial states (IS), the corresponding transition states (TS) and final states (FS) of on the Ru(0001) surfaces, along with the adsorption energies (E_{ads}). H: white; C: grey; O: red; Ru: cyan.

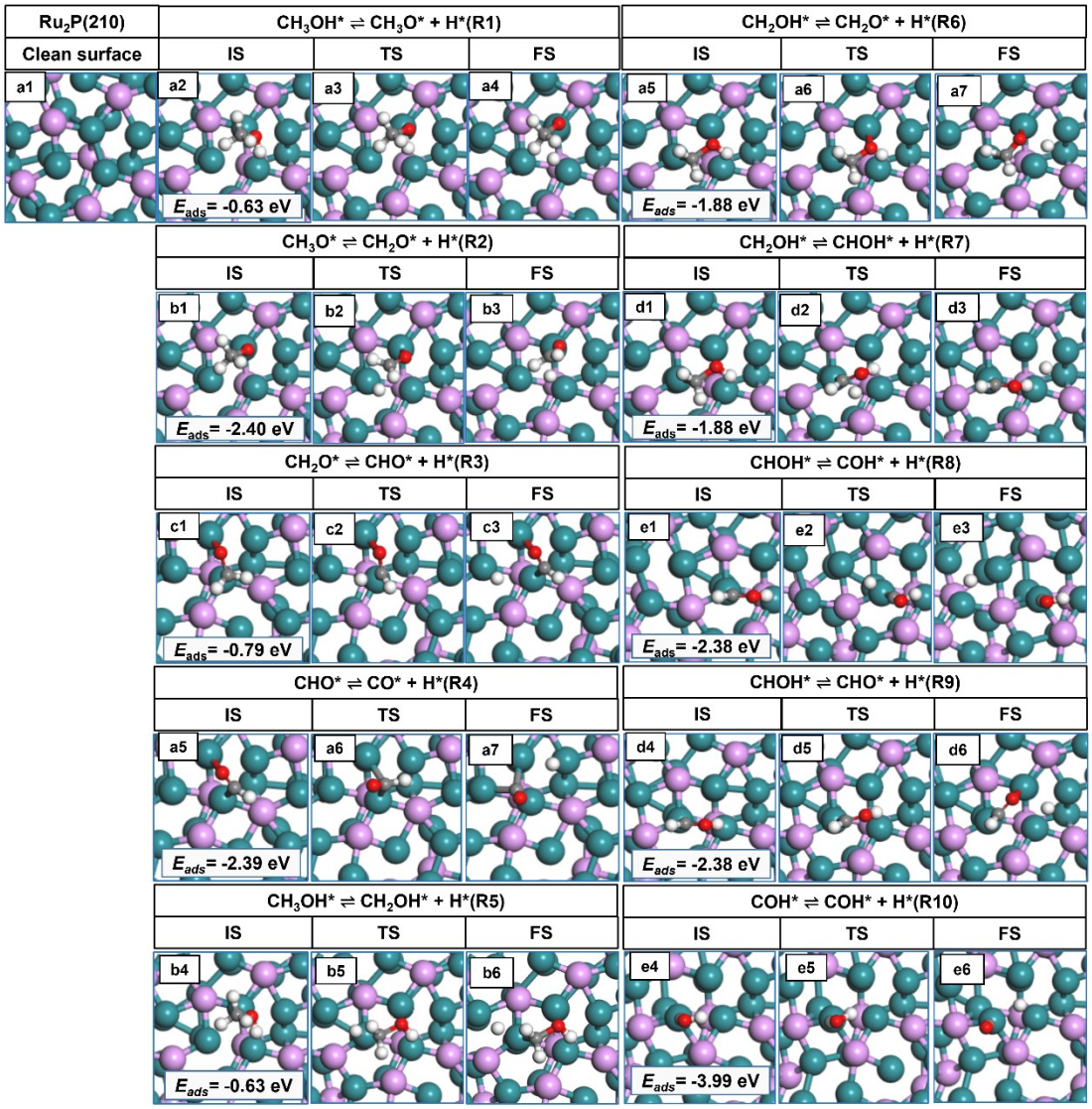

Figure S4. Top view of all the initial states (IS), the corresponding transition states (TS) and final states (FS) on the $Ru_2P(210)$ surfaces, along with the adsorption energies (E_{ads}).H: white; C: grey; O : red; P: purple; Ru: cyan.

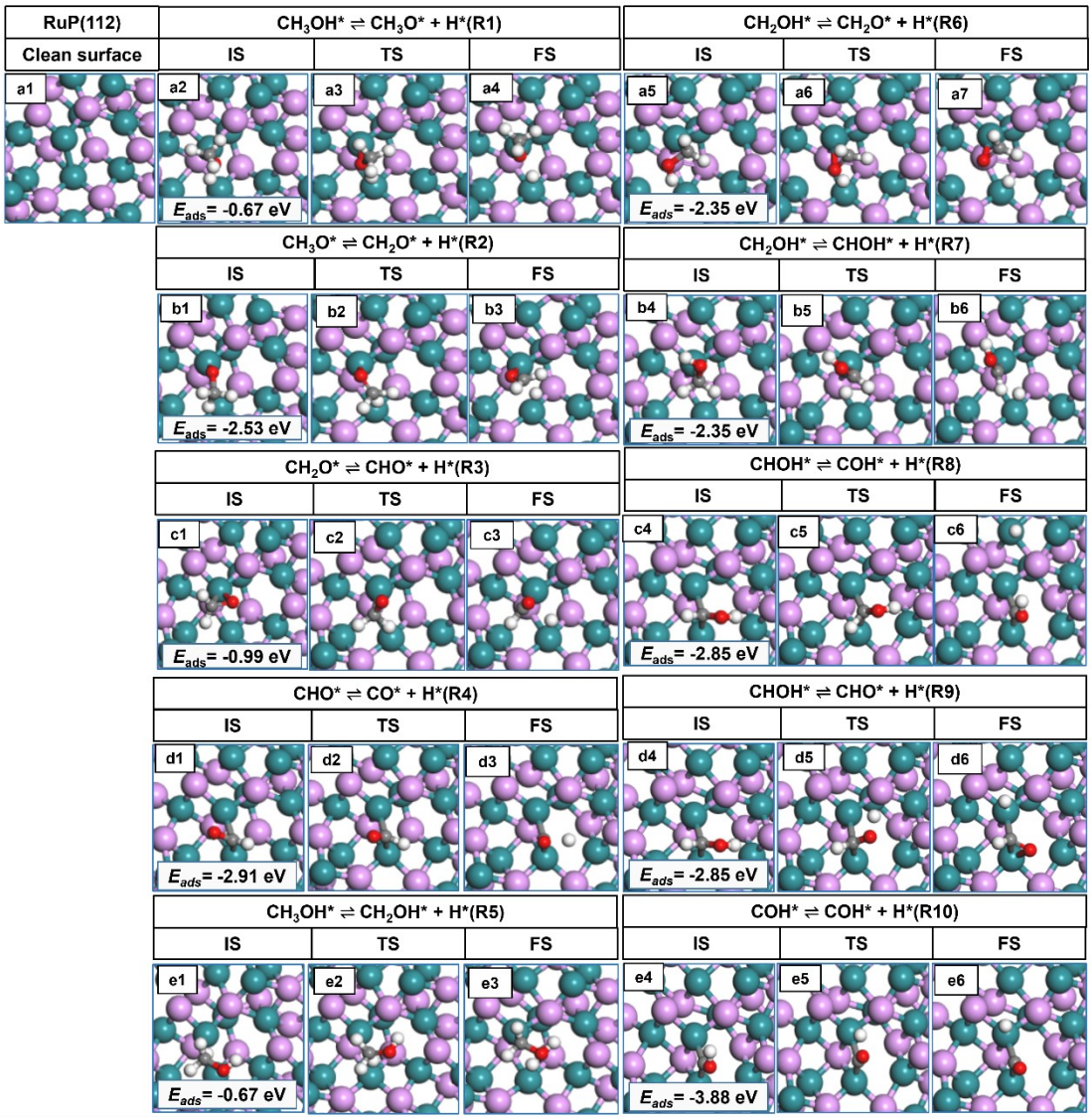

Figure S5. Top view of all the initial states (IS), the corresponding transition states (TS) and final states (FS) on the RuP(112) surfaces, along with the adsorption energies (E_{ads}).H: white; C: grey; O : red; P: purple; Ru: cyan.

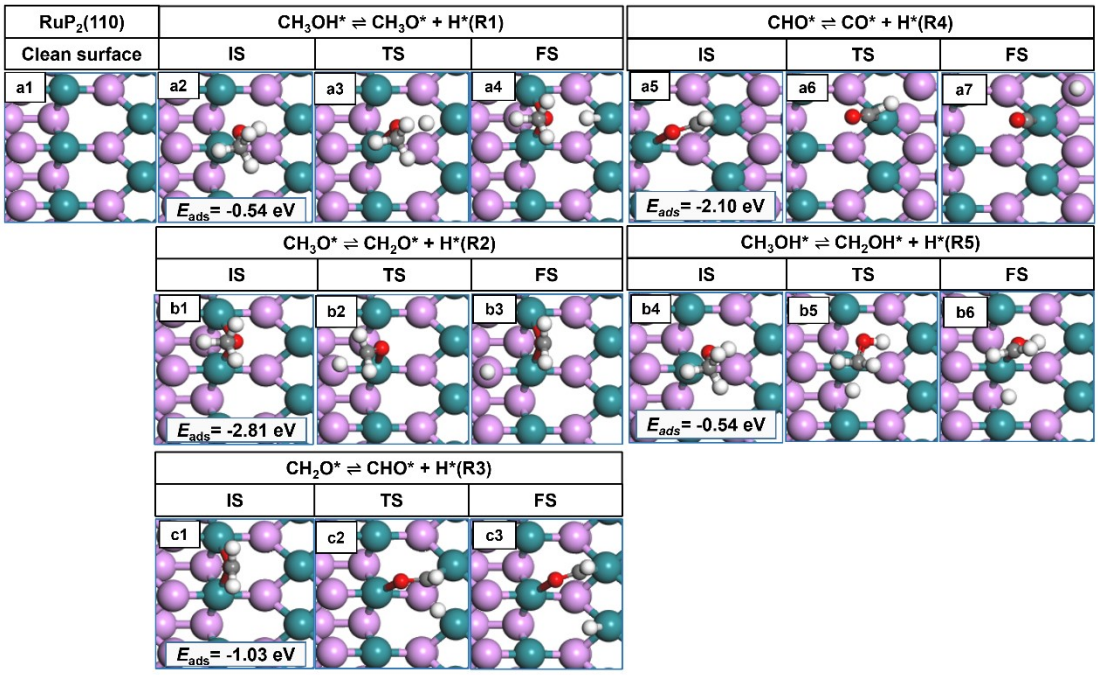

Figure S6. Top view of all the initial states (IS), the corresponding transition states (TS) and final states (FS) on the $RuP_2(110)$ surfaces, along with the adsorption energies (E_{ads}).H: white; C: grey; O : red; P: purple; Ru: cyan.

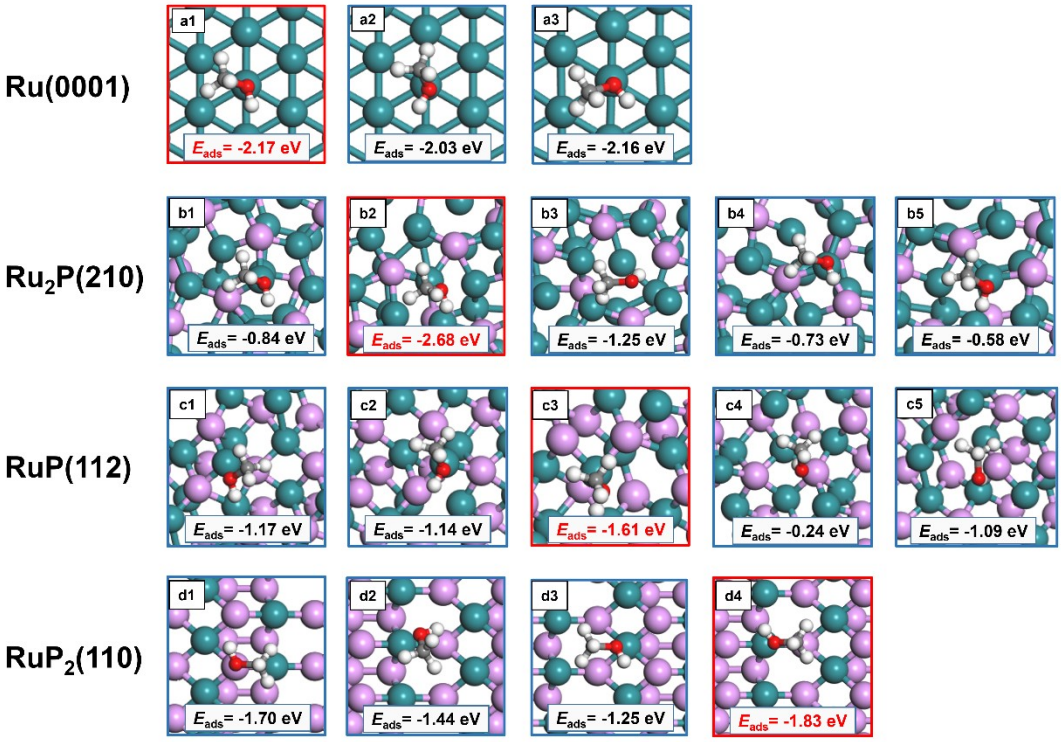

Figure S7. Screening of methanol adsorption sites on Ru(0001), $Ru_2P(210)$, RuP(112), and $RuP_2(110)$ surfaces (To save computing resources, the K-point of 1×1×1 is used for adsorption site screening). H: white; C: grey; O: red; P: purple; Ru:

cyan.

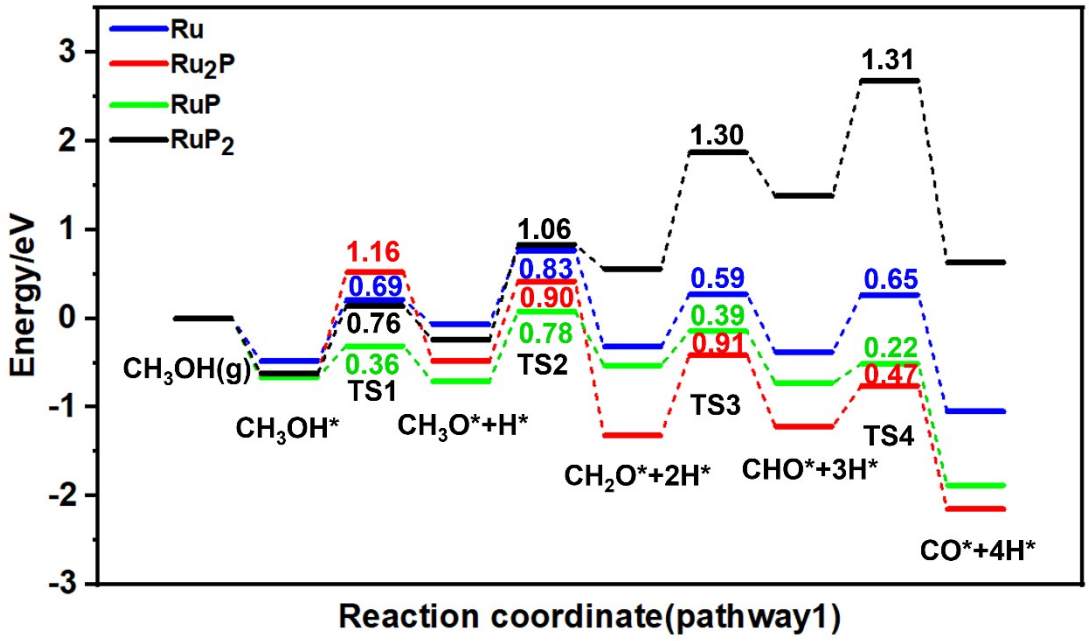

Figure S8. Reaction energy barriers for pathway 1 on the Ru_xP_y surfaces.

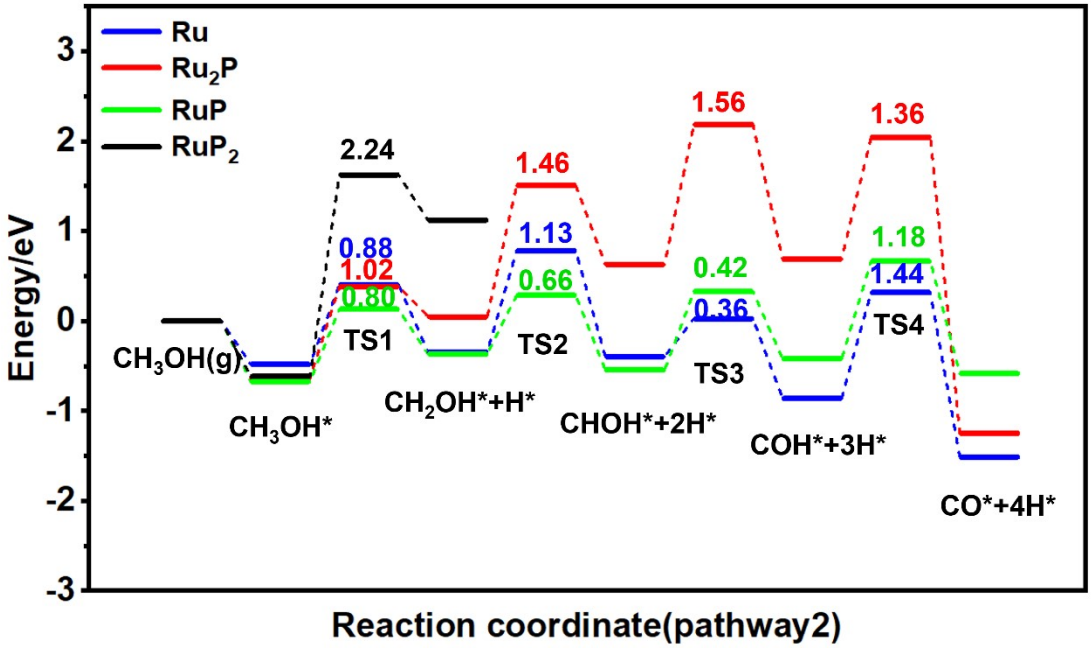

Figure S9. Reaction energy barriers for pathway 2 on the Ru_xP_y surfaces.

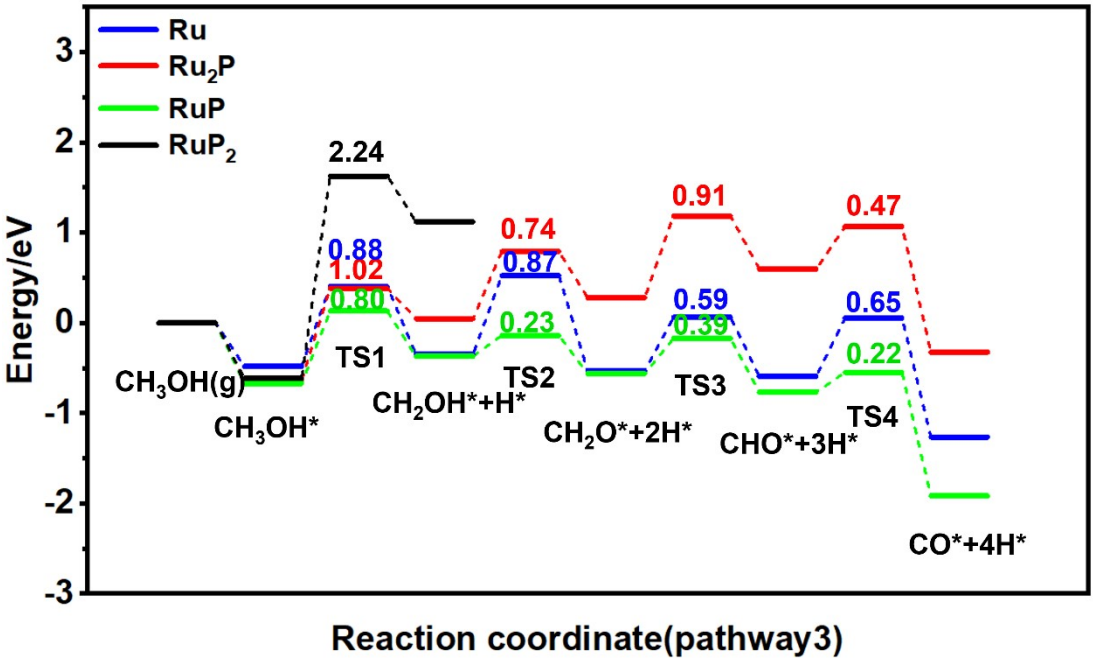

Figure S10. Reaction energy barriers for pathway 3 on the Ru_xP_y surfaces.

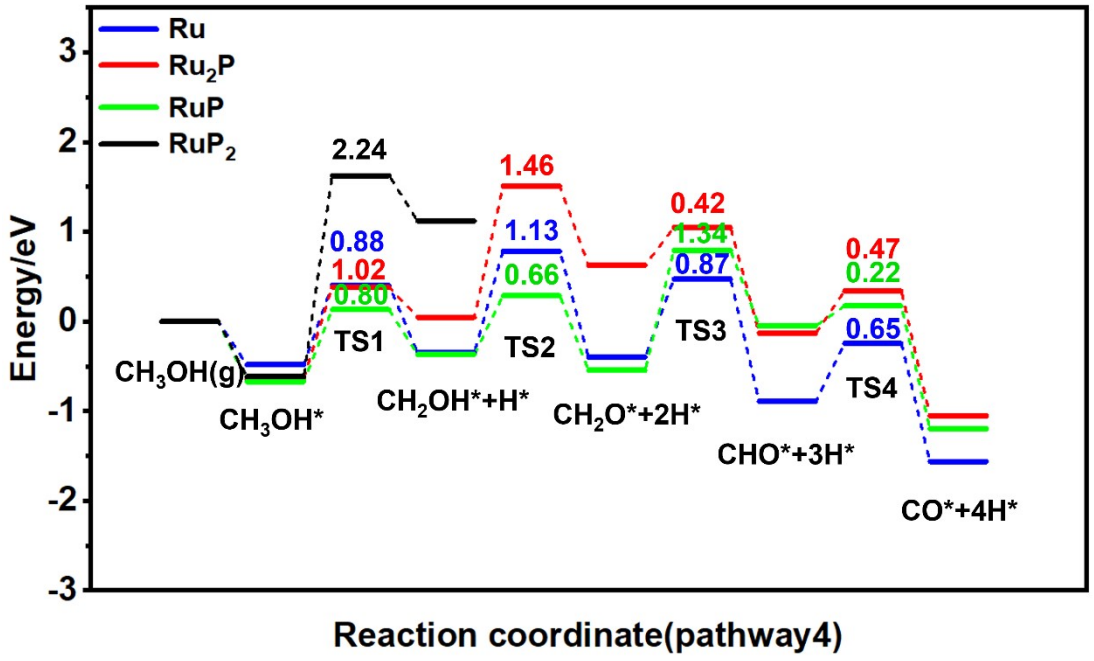

Figure S11. Reaction energy barriers for pathway 4 on the Ru_xP_y surfaces.

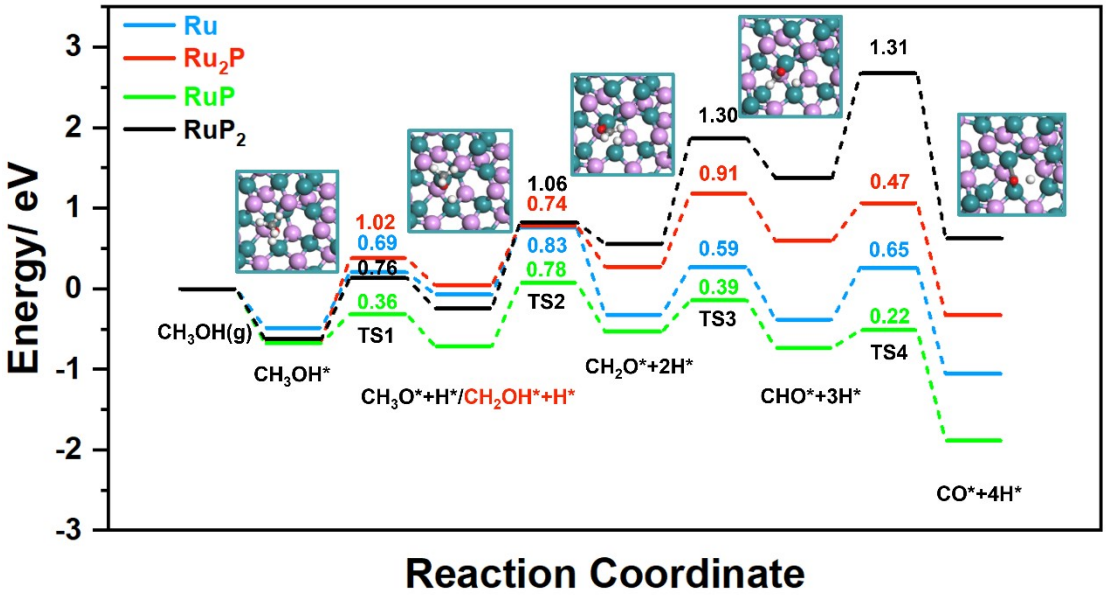

Figure S12. Optimal pathways for methanol dehydrogenation on Ru(0001) (pathway1), Ru_2P(210) (pathway3), RuP(112) (pathway1), and RuP_2(110) (pathway1) surfaces, respectively.

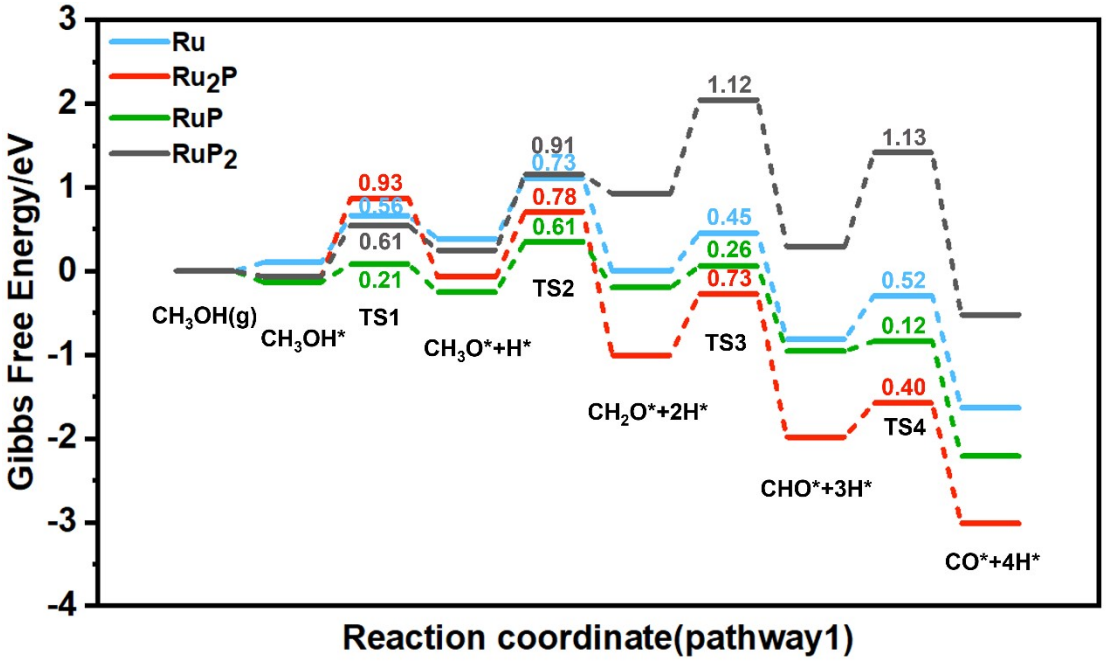

Figure S13. Reaction free energy barriers for pathway 1 on the Ru_xP_y surfaces.

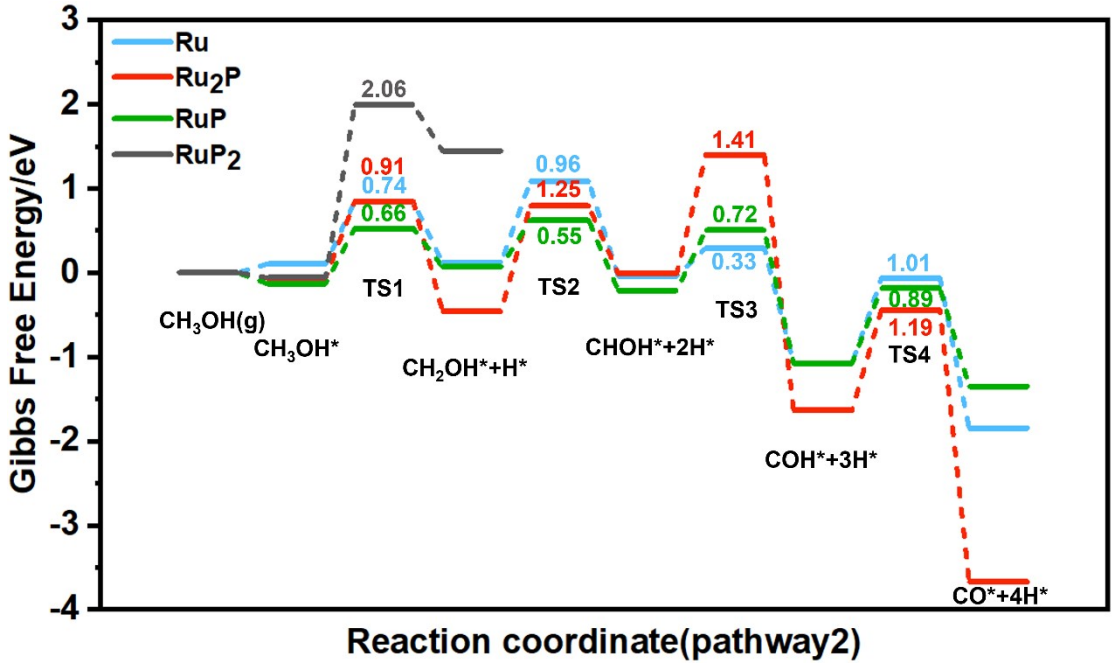

Figure S14. Reaction free energy barriers for pathway 2 on the Ru_xP_y surfaces.

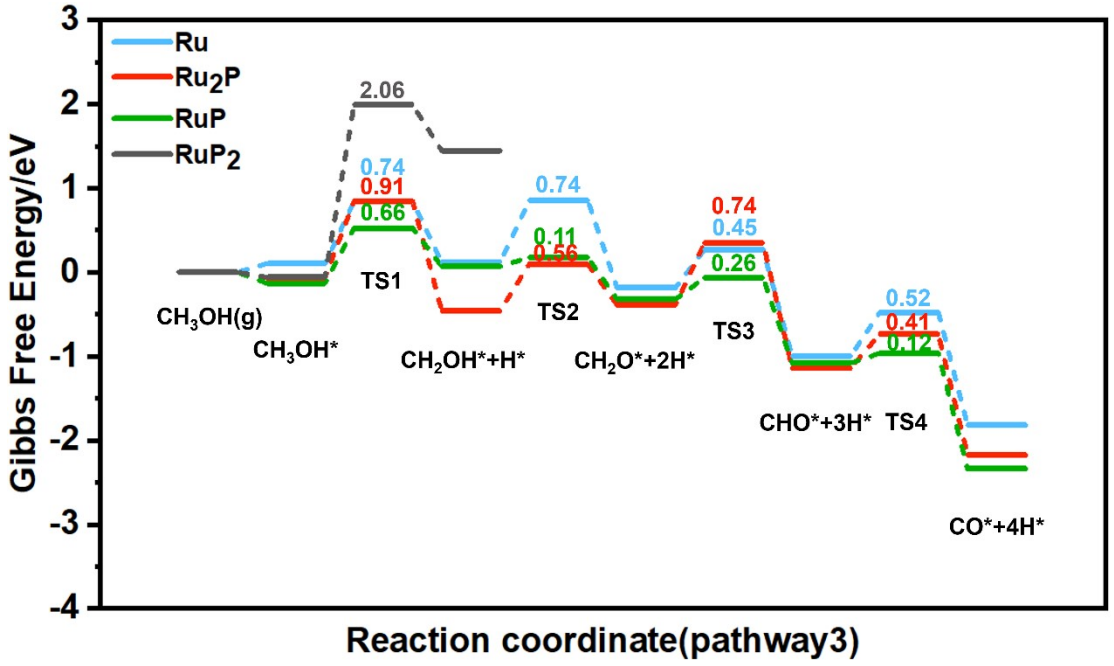

Figure S15. Reaction free energy barriers for pathway 3 on the Ru_xP_y surfaces.

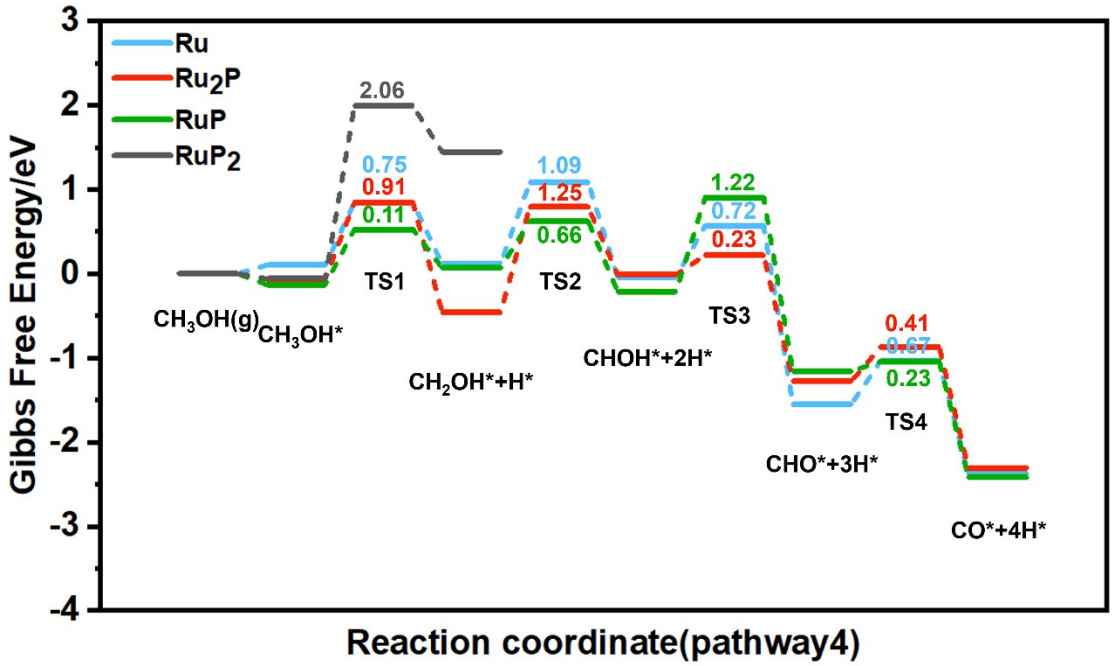

Figure S16. Reaction free energy barriers for pathway 4 on the Ru_xP_y surfaces.

Table S7. The states of TDTS and TDI, the energies of TDTS and TDI, and the calculated E_a^{eff} of MD over the surfaces of Ru(0001), Ru_2P(210), RuP(112), and RuP_2(110).

	Ru(0001)	Ru_2P (210)	RuP(112)	RuP_2(110)
TDTS	TS4	TS3	TS2	TS4
E_{TDTS} (eV)	0.76	1.19	0.08	2.68
TDI	CH_3OH*	CH_3OH*	CHO*+3H*	CH_3OH*
E_{TDI} (eV)	-0.48	-0.63	-0.70	-0.62
ΔE	0	0	0	0
E_a^{eff} (eV)	1.24	1.82	0.78	3.30

Table S8. Comparison of previous DFT calculations works on the mechanism of MD reaction over metal-based catalysts (without support).

Catalyst	Calculation software	Advantage Path	RDS energy barrier (electronic energies)	Reference
RuP(112) Ru(0001)	VASP	$CH_3OH \rightarrow CH_3O \rightarrow CH_2O$ $\rightarrow CHO \rightarrow CO$,	0.78 eV, 0.83 eV	In this work

		$CH_3OH \rightarrow CH_3O \rightarrow CH_2O \rightarrow CHO \rightarrow CO$		
Ru(0001)	DMol^3	$CH_3OH \rightarrow CH_3O \rightarrow CH_2O \rightarrow CHO \rightarrow CO$	1.01 eV	29
Pd(100)	CASTEP	$CH_3OH \rightarrow CH_2OH \rightarrow CHOH \rightarrow CHO \rightarrow CO$	1.79 eV	11
Rh(111)	DMol^3	$CH_3OH \rightarrow CH_3O \rightarrow CH_2O \rightarrow CHO \rightarrow CO$ and $CH_3OH \rightarrow CH_2OH \rightarrow CHOH \rightarrow CHO \rightarrow CO$	0.72 eV	14
Pd(111), Pt(111), Ni(111)	VASP	$CH_3OH \rightarrow CH_2OH \rightarrow CHOH \rightarrow CHO \rightarrow CO$, $CH_3OH \rightarrow CH_2OH \rightarrow CHOH \rightarrow CHO \rightarrow CO$, $CH_3OH \rightarrow CH_2OH \rightarrow CHOH \rightarrow CHO \rightarrow CO$	0.66 eV, 0.62 eV, 0.74 eV	15
PdAu(100)	DMol^3	$CH_3OH \rightarrow CH_3O \rightarrow CH_2O \rightarrow CHO \rightarrow CO$	1.41 eV	26
PtRu/Pt(111)	DMol^3	$CH_3OH \rightarrow CH_3O \rightarrow CH_2O \rightarrow CHO \rightarrow CO$	1.10 eV	27